

Article

Airflow Field Around *Hippophae rhamnoides* in Alpine Semi-Arid Desert

Lihui Tian ¹, Wangyang Wu ^{2,*}, Dengshan Zhang ¹ and Yang Yu ³

¹ State Key Laboratory of Plateau Ecology and Agriculture, Qinghai Academy of Agricultural Forestry Sciences, Qinghai University, Xi'ning 810016, China; lhtian@qhu.edu.cn (L.T.); dshzhang@bnu.edu.cn (D.Z.)

² School of Earth Sciences, East China University of Technology, Nanchang 200237, China

³ Department of Sediment Research, China Institute of Water Resources and Hydropower Research, Beijing 100038, China; theodoreyy@gmail.com

* Correspondence: wuwangyang@ecit.cn

Received: 10 April 2020; Accepted: 4 May 2020; Published: 6 May 2020



Abstract: The research on wind regimes and the wind protection mechanism of sand-fixing plants has mainly relied on wind tunnel experiments; few observations have been made in the field. At the same time, airflow around individual standing vegetation elements and communities is relatively lacking in alpine semi-arid deserts. Therefore, this paper selected 10-year-old *Hippophae rhamnoides* (sea buckthorn) on sandy land on the eastern shore of Qinghai Lake as the study object. Based on spatial and temporal changes of wind regime in the afforestation forest, a structural simulation of airflow near the plant and at different layers above the ground, and the annual changes in wind protection, we studied the wind protection mechanisms of *H. rhamnoides* as single elements or communities. The results were as follows: the effective protection length of the sublayer of *H. rhamnoides* was 1.0 to 1.8 m. The higher the layer, the smaller the decrease in wind velocity behind elements, and the smaller the effective protection length. Wind velocity downwind of *H. rhamnoides* increased, with height increasing where the airflow decreases rate (R) decreased in the sublayer, and increasing in the middle layer as plant height increased. Meanwhile, the airflow decreases rate (R) was negative in the upper layer because it decreased as the plant height increased. The airflow movement between elements had various directions because the upper layer was prone to fluctuations due to the swinging of the crown and branches, and turbulence was seen at the sublayers owing to the mechanical resistance of the elements. When the wind speed at the standard point was 8.5 m/s and the wind direction was east (E), the increase of airflow velocity at the side and center in the upper layer was more significant, and there was a strong wind zone in the azimuth of NW-N-NE-E-SE, while the S-SW-W azimuth zone was weaker. The sand-fixing shrub *H. rhamnoides* had a significant windproof function, and the 1.5 m square interval density of *H. rhamnoides* was suitable for alpine desert control projects.

Keywords: alpine semi-arid desert; *Hippophae rhamnoides*; wind flow; airflow decreases rate; effective protection length

1. Introduction

Vegetation can greatly reduce the wind erosion rate and plays an important role in soil wind erosion and desertification control in arid and semiarid regions [1,2]. Vegetation acts to reduce soil loss by wind in three ways: firstly, the vegetation shelters the soil from the erosive force of the wind by covering a proportion of the surface. Secondly, vegetation reduces the force of the wind near the ground by extracting momentum from the wind at a height above the surface. Finally, vegetation traps soil particles in transport, thereby encouraging sediment deposition [3,4]. Plants cut off airflow

so that airflow fields decay dramatically [5,6], and the erosion rate decreases significantly around plants [7]. However, much research has been done on the effects of windbreaks and natural shelterbelts on wind speed, while not much research has been done on the effect of single shrubs on wind speed [6]. Moreover, previous research mainly focused on the quantitative study of the airflow field around plants [8] and variation in the speed of airflow along the airflow direction in the downwind vegetation in wind tunnel experiments, but not with real plants [5,6]. This showed that airflow fields around plants were partitioned into three parts: a mild deceleration area in the upwind region [9], acceleration areas on both sides [8], and the wake deceleration area in the downwind region [5]. The wake deceleration area has received major research interest due to its influence on vegetation characteristics such as wind speed variation, turbulence [5], and eddies [10] along the wake axis [11,12]. No matter the natural vegetation or anthropogenic vegetation, wind speed variation in the wake area directly affects the windproof distance and effects [13]. Therefore, a comprehensive understanding of the airflow field patterns around plants is needed to investigate the dynamic mechanisms of soil erosion of a vegetation-covered ground surface in the field.

The characteristics of wind regime and the wind protection mechanisms of vegetation have regional variations in different deserts [14,15]. Scientists have analyzed the relationships between plant cover, surface roughness, and wind shear stress from the perspective of aerodynamics, and built aerodynamic models and surface sediment transport models under different vegetation conditions [8,11,16]. Shrubs form a special class of obstacles referred to as “vegetated obstacles” [17]. Shrubs allow air to pass through the obstacles and considerably complicate the modeling of the airflow [10]. The flow around vegetated obstacles is a secondary, three-dimensional structure, with separation occurring in both the horizontal and vertical planes [17]. Factors such as the coverage, distribution, lateral coverage, and height to-width ratio of vegetation alter the spatial distribution of the airflow field on vegetation-covered surface [8,11,18–20], and this spatial distribution is extremely uneven [12]. The spatial distribution of the airflow field on a vegetation-covered surface is affected not only by the characteristics of a single plant but also by the arrangement and density of the plants [21,22]. However, there are few studies focused on airflow fields around vegetation growth in the field, especially sand-fixing shrubs, which make up the largest proportion of afforestation vegetation in desertification control projects. Sand-fixing plants not only block upwind airflow and force the energy of airflow to be dispersed and reduced, but also prevent airflow from concentrating on the ground. The reduction of wind energy means sand is difficult to move on the soil surface, which blocks sand from entering into the air, achieving benefits in the form of wind-breaks and sand fixation.

Qinghai Lake is located in the northeast of the Qinghai-Tibet Plateau and belongs to an alpine semi-arid ecological fragile district and a global climate change-sensitive area. The rise in the lake water level, global warming, and the implementation of desert prevention and control projects reduced the area of desertified land around the Qinghai Lake basin. During the past 10 years, from 2008 to 2017, all forest land formed a vegetation community dominated by plants, and large-scale mobile sand dunes were gradually transformed into semi-fixed or fixed dunes [23]. Plants have effectively reduced wind and sand hazards in this area, and have played an important role in the traffic of East Lake Road and the Qinghai-Tibet Railway. However, research on wind protection mechanisms and the ecological functions of sand-fixing plants in alpine desert has only been on the benefits of some farmland windbreaks and holistic ecological effects [24–26], while long-term observations of the airflow structure and wind protection function of typical sand-fixing plants has been absent; meanwhile, knowledge of the features of airflow around individual plants and communities is also lacking. Therefore, it is significant to study the windproof mechanisms of sand-fixing plants and ecological interactions between the atmosphere and vegetation through field observations of airflow in planted areas in alpine semi-arid desert with greater annual wind speed, higher wind frequency, and variable wind direction.

As a sand-fixing shrub, *Hippophae rhamnoides* (sea buckthorn) has been growing in the Qinghai Lake desert for more than 30 years [24,26]. It has the largest proportion of all the sand-fixing plants in this area. Therefore, this paper selected 10-year-old *H. rhamnoides* planted on sandy land at the eastern

shore of Qinghai Lake as the study object. According to temporal and spatial changes of the wind in the shrubs, we made a structural simulation of the airflow field around a single plant and at different layers above the ground, as well as the annual changes in wind protection function, to explore the mechanism of wind protection in restoration areas in the alpine desert. This will effectively guide our study of the ecological adaptation process, species selection, and structural optimization of plantings in the alpine desert.

2. Materials and Methods

2.1. Study Area

The study was conducted in the Ketu Wind Prevention and Sand Fixation Experimental Range (hereafter, WPSE; $36^{\circ}40' N$, $100^{\circ}45' E$, 3224 m elevation a.s.l. (above sea level)) in the southeast corner of Haiyan Bay, surrounded by the Ruiyue and Tuanbao Mountains on the eastern shore of Qinghai Lake (Figure 1). Megadunes and continuous mobile dunes are distributed in WPSE. The area of Ketu Sandy Land is about 753 km², which is the largest area on the eastern shore of Qinghai Lake and is severely desertified land. The study region was a low wind energy environment that had the strongest aeolian activity from late autumn to early spring, controlled by the NW direction of the wind [27]. The threshold wind velocity for sand movement on a mobile dune was 6.5 m/s, while it was greater than 8 m/s on afforestation dunes [27].

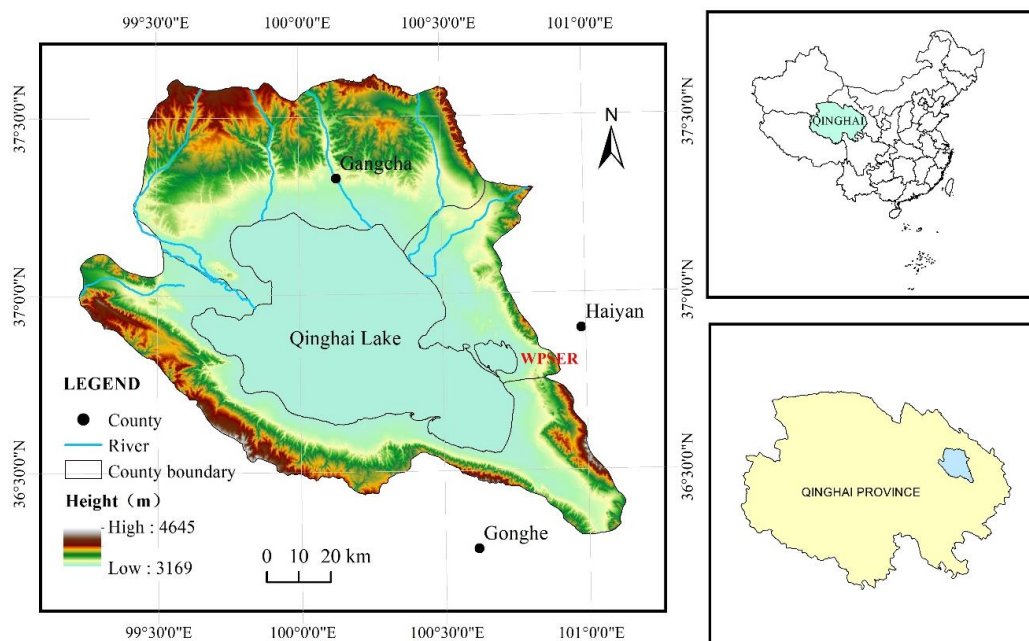


Figure 1. Geographic location of the study area.

Since the WPSE was established in 2008, afforestation coverage has increased at a rate of 6.40% to 8.80% per year. Community coverage was up to 75% in the summer. The wind protection effectiveness for eight- to 10-year-old *H. rhamnoides*, *Salix cheliophe*, *Populus sylvestris*, and *Pinus sylvestris* could be more than 50%, and the sand-fixing efficiency was more than 85% [23]. The study showed that decreasing sand transport was closely related to an increase in vegetation coverage owing to afforestation in this area [28]. *H. rhamnoides* was planted in 2008, and had an average height of 1.0 m and the afforestation specification was 1.5×1.5 m in WPSE.

We used meteorological data from Haiyan Weather Station, 30 km from WPSE, to represent the wind regime for the study region. The average annual wind speed in the past 10 years was 3.0 m/s to 3.5 m/s. The wind direction was variable but had two main sectors: the first was a northwest (NW) wind in the winter and the other was a southeast (SE) wind in summer; wind speed in winter was

significantly higher than in summer. In addition, windy seasons were relatively longer, with a high frequency of strong winds from November to April each year (Figure 2).

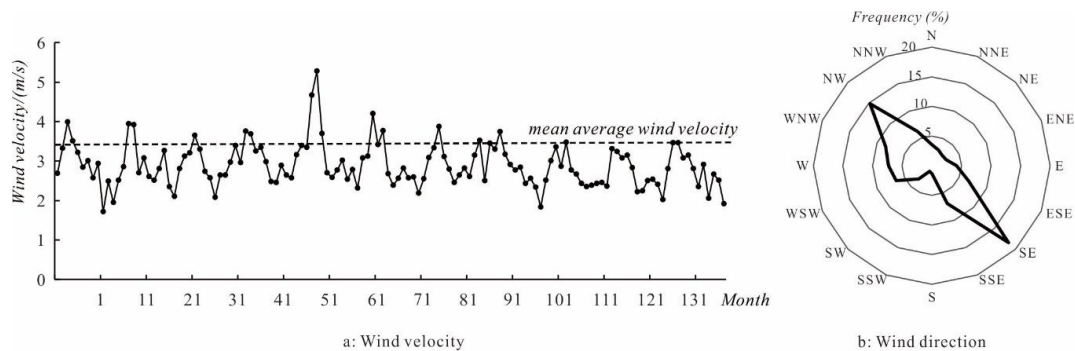


Figure 2. The annual average wind speed (a) and wind direction (b) of Haiyan Weather Station in the past 10 years (2006 to 2016).

2.2. Study Methods

In April and August of 2016 and 2017, at the top of dunes where *H. rhamnoides* was planted, we observed the wind velocity and direction for individual plants using a ZK-BX5A handheld meteorological instrument with a ranging rope, self-made wind speed rack, one 2.5-m-high main pole, four side poles of different heights (0.5, 1.0, 1.5, and 2.0 m), and PVC pipe height marks. At the same time, we measured three layers of airflow field for 1-m-high *H. rhamnoides* (sublayers: 0.1 and 0.2 m, middle layers: 0.5 and 1.0 m, upper layers: 1.5 m, average of two heights for sublayers and middle layers) to analyze the airflow change downwind of the plants at different layers.

We selected three different heights of *H. rhamnoides* (0.5, 1.0, 1.5 m) to observe the airflow field change for different plant heights. During the measurements, we took down the wind velocity at a height of 2 m in flat and non-distorted environments (V_m) as a standard point that provided reference wind data against which mobile anemometry data could be normalized [6]. Practicality constraints meant that data collected at the height of each vegetation element were normalized against reference data measured at 2 m height (the normalization of wind velocities at multiple heights using a single reference height is common practice) [29]. Mobile points at different positions around plants (V_n) were continuously observed for 10 min at each observation time as horizontal flow points (Figure 3a). Three plants of the same height were selected for repetition. According to the four vertical heights of airflow frame (0.5, 1.0, 1.5, and 2.0 m), each horizontal flow point was observed four times simultaneously. The seven points behind the plant were the downwind length ($L = 0.25 H, 0.5 H, 1.0 H, 1.5 H, 2.0 H, 4.0 H, 8.0 H$, where H is the plant height). In addition, in order to draw an airflow diagram, one point in front of the plant (0.5 H upwind) and six points located 0.5 m from the sides of the plant were set (Figure 3a). When measuring wind velocity at each point, the wind speed at the standard point (V_m) must be greater than 3 m/s because the mean annual wind velocity in this area was 3.0 to 3.5 m/s. When the wind speed at the standard point was 6.5 m/s and the wind direction was northeast to east (NE-E), the distribution of the airflow velocity and direction between adjacent plants was seen to differ between locations and layers.

Moreover, three 5×5 m plots were selected at the top of dunes to measure the airflow of the upper layer (2 m) and lower layer (0.5 m) in the spring, summer, and autumn of 2017 to assess the seasonal differences in airflow fields. The measurement points included eight points distributed around the plants and the center point between the plants (Figure 3b); wind speed and direction data were recorded at a frequency of 1 min, and two layers were monitored simultaneously. *H. rhamnoides* was planted in 1.5-m squares in the study area, so the spacing was 1.5 m for each single plant.

The airflow decreases rate (R), also called the minimum relative wind speed, is the ratio of the minimum wind speed at point D in the lee to the wind speed at the reference point D_0 :

$$R = \frac{V(i, D_0) - V(i, D)}{V(i, D_0)} \times 100\% \tag{1}$$

where $V(i, D_0)$ is the wind velocity at 0.5 m in front of the plant. i represents different layers (sublayers: 0.1 and 0.2 m, middle layers: 0.5 and 1.0 m, upper layers: 1.5 m). $V(i, D)$ is the lowest wind velocity downwind of the plant at same height to D_0 . D is the point at which the lowest wind velocity is in downwind of the plant.

Meanwhile, the maximum windproof length (L_{max}) represents the distance at which the airflow velocity in the lee side of the plant first recovered to the same height as the front of the plant. It is beneficial to reflect the relationship between effective protective distance and height of plant, in order to guide the density of plant arrangement. Because the field data have only five height levels and six horizontal distance points, we took 0.5 m in front of the plant as the initial wind speed point. It was common to have insufficient sample points and a low fitting accuracy of the curve.

We used Origin 9.0 software (OriginLab Cor., Northampton, MA, USA) to draw the airflow distribution diagram and illustrate the eight orientation distributions in different seasons.

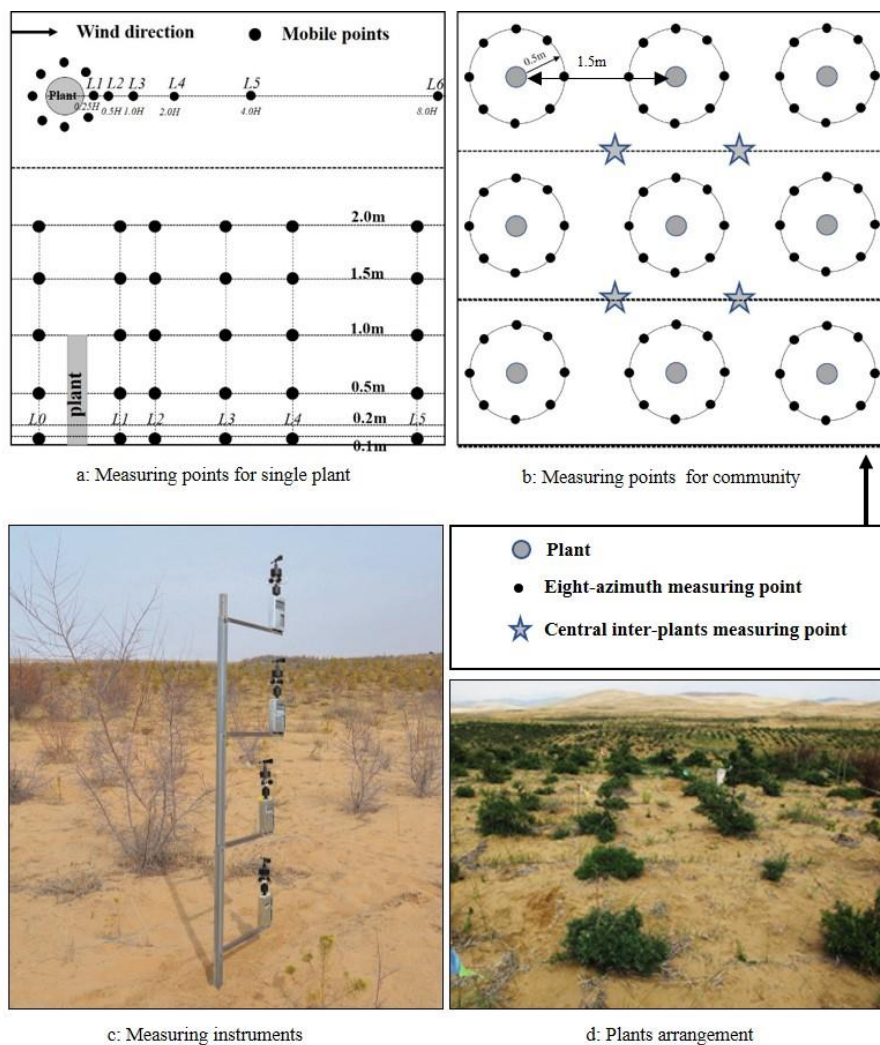


Figure 3. Measuring points for individual plants (a) and between plants (b), as well as the measuring instruments (c) and plant arrangement (d).

3. Results

3.1. Airflow behind the Plants

According to the airflow change features of *H. rhamnoides* plants in spring 2016, when the wind speed at the standard point (V_m) was 8 m/s, the airflow around plants at different layers was significantly different in the downwind zone and the space directly surrounding *H. rhamnoides* (Figure 4). The wind velocity of the sublayer was low and the lowest velocity appeared at L (length behind the plant) 0.15 to 0.55 m; the velocity was about 35% to 70% of that in the frontal zone, and the maximum effective protection length (L_{max}) was 1.8 m. While airflow velocity fluctuated in a low amplitude at the middle layer, the lowest and second-lowest values appeared at 0.3 to 0.5 m and 3 m behind the plant, respectively. The velocity behind the plant was 75% to 85% of that at the front zone, the same as 1 m behind the plant.

The wind velocity downwind of the upper layer was larger than that at the front zone. Peaks and valleys appeared near the vegetation crown and 1.5 m above the ground behind the plant, and then increased sharply. This showed that the effective wind protection distance of the sublayer of *H. rhamnoides* was 1.0 to 1.8 m. The higher the layers, the smaller the rate of the decrease in velocity and the lower the effective protection length behind plants. In addition, 2 m behind the plants, peaks and valleys of airflow velocity appeared in the middle and upper layers, respectively, which reflected air vortices 2 m behind the plant and 1 m above surface.

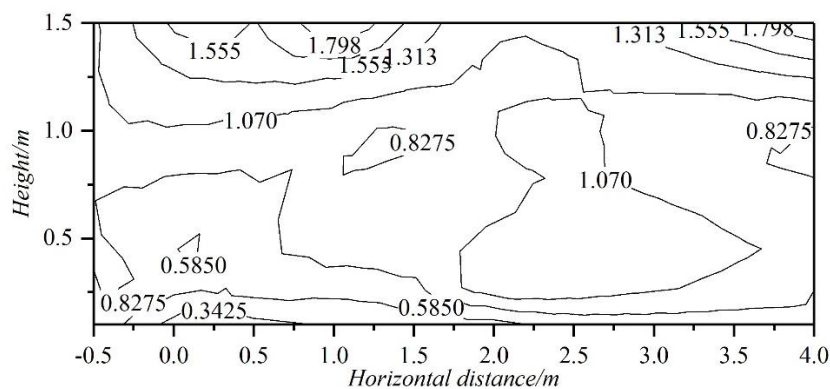


Figure 4. Airflow distribution at different heights behind 1-m-high *H. rhamnoides* (contour value was V_n/V_m , V_n is wind velocity of mobile points at different positions around plants, V_m is wind speed at the standard point).

There were significant differences in the plant height and crown width of the same sand-fixing species that influenced the airflow features of windward plants. The airflow velocity of *H. rhamnoides* increased as the plant height increased, but the decrease rate of airflow velocity (R) showed significant differences between layers (Figure 5). The decrease rate of airflow velocity (R) in sublayers decreased with the increase in plant height, while it increased in middle layers. However, the airflow increase rate decreased with the increase in plant height (Table 1). For the effective protection length (L_{max}), the middle layers were always larger than the sublayers, and upper layers were continuously increasing as the plant height of each layer increased. There was a large difference in airflow velocity between the middle and upper layers for 1.5-m-high *H. rhamnoides*, which created a low vortex behind plants, and the maximum protection distance was increased to 5 m in the middle layers. At the same time, the protective length of the upper layers became smaller since it was easy to form an accumulation area near the crown.

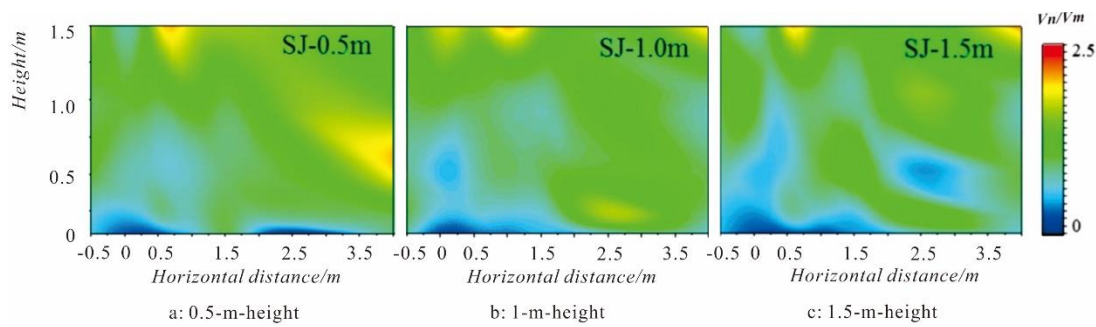


Figure 5. Airflow distribution for 0.5-m-height (a), 1-m-height (b) and 1.5-m-height (c) of *H. rhamnoides*.

Table 1. The airflow decreases rate (R) and maximum windproof length of airflow (L_{max}) for different heights of *H. rhamnoides*.

Height (m)	The Airflow Decreases Rate (R)/%			Maximum Windproof Length (L_{max})/m		
	Sublayers	Middle layers	Upper Layers	Sublayers	Middle Layers	Upper Layers
1.50	45.42	31.70	−1.75	1.95	5.00	0.90
1.00	69.35	19.74	−69.53	1.30	1.90	2.10
0.50	45.58	10.28	−76.36	0.90	1.40	0.00

3.2. Airflow between the Communities

It was beneficial to explore the wind protection mechanisms of the plant community and micro differences in the erosivity of the wind by studying the wind velocity and direction in the upper (2 m) and lower layers (0.5 m) of *H. rhamnoides*. Airflow movement between plants had a directional change: the upper layer was prone to fluctuating forward due to the swinging of the crown and leaves, while the lower layer was turbulent owing to mechanical barriers of plants. According to field observations (Table 2), the airflow movement direction of the upper layer of *H. rhamnoides* was E-ESE-SE when the direction of the incoming wind was NE-ENE-E. It was deflected clockwise by 75° to 85° and amplitude at the side followed by behind and center of communities. In the lower layer, the airflow was SE in all directions with mainly clockwise deflection, and the angle of forward and backward flow was 100° to 105°.

Table 2. Airflow velocity (V_i , m/s) and direction (D_i , °) in different layers of *H. rhamnoides* communities.

Layers	V_f	D_f	V_a	D_a	V_b	D_b	V_c	D_c
0.5 m	5.84	124	5.20	118	4.19	105	5.42	102
2.0 m	2.96	129	2.83	139	2.13	146	2.64	141

Note: V_f , V_a , V_b , and V_c are the wind velocity of the frontal zone, at the side, behind the plant, and at the center of communities, respectively. D_f , D_a , D_b , and D_c are the wind direction of the frontal zone, at the side, behind the plant, and at the center of communities, respectively.

The velocity of airflow around plants on sand dunes showed certain azimuth differences and spacing effects. When the wind speed in standard point was 8.5 m/s and the wind direction was from the east, we compared the airflow distribution of the lower and upper layers (Figure 6). The upper layer’s side and central airflow increased more significantly than that of the lower layer. The direction of the NW-N-NE-E-SE azimuth zone formed a strong interplant wind zone, while the S-SW-W azimuth zone had a weaker airflow velocity. The wind velocity of the lower layer was lower than that of the upper layer on the whole, and the airflow velocity in the leeward azimuth zone (W-SW-S) was particularly weak.

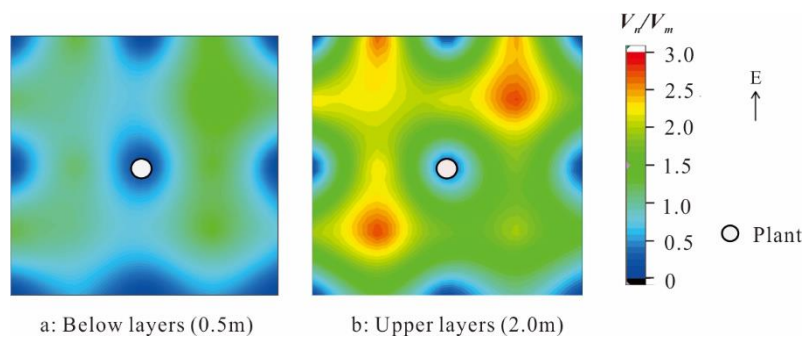


Figure 6. Airflow distribution of below layers (a) and upper layers (b) of the *H. rhamnoides* community.

3.3. Eight-Azimuth Airflow Around the *H. Rhamnoides* Plants

The airflow distribution structure of a single element was the basis for analyzing characteristics of airflow movement in a plant community, and was also the internal mechanism of differences in the intensity of soil erosion under plants and patterns of nebkha morphology. When the wind speed at the standard point was 6.5 m/s we measured the airflow distribution of *H. rhamnoides* communities in different seasons. According to Figure 7, it had the following characteristics: (1) the airflow velocity of the frontal zone (in front of the plant) was about 1.5 to 5.5 times higher than that of the leeward zone (behind the plant). (2) The wind velocity around the side of an individual plant was 1.0 to 4.5 times higher than that downwind, and that of the lower layer was higher than that of the upper layer. (3) The difference between the wind velocity in front of the plant and around the side was small; the velocity in front of the plant was slightly larger than that around the side in the upper layer, especially in the autumn. (4) Airflow velocity azimuth difference was relatively significant in each season, and that of the upper layer was larger than that of the lower layer.

There was little difference between different positions surrounding the single elements of the wind direction. The angle changed from 0° to 90° and lower layer > upper layer, as well as behind > side > front. The dominant wind direction changed with the season in the study site, being N-NE in spring, SE-S in summer, and W-NW in autumn. As a result, the front and side of plants were more affected by the wind direction, the same as the standard point; the side was slightly smooth, while the area behind was affected by multidirectional airflow, which had weak wind velocity and an unstable wind direction.

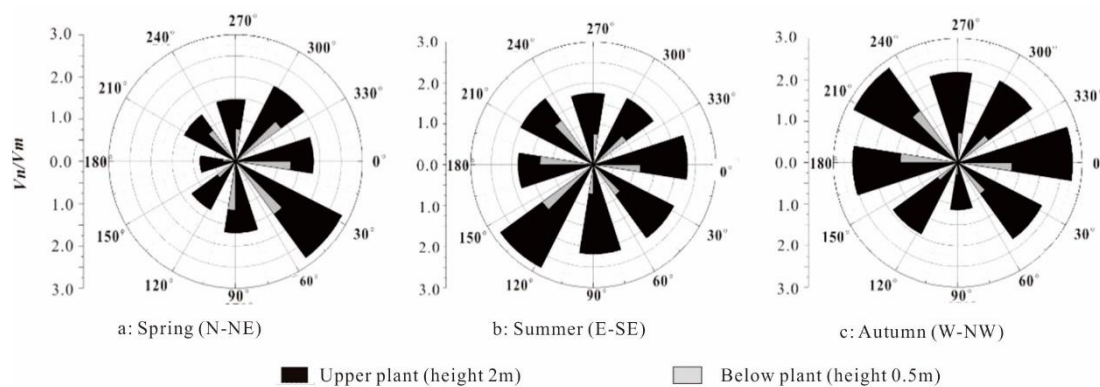


Figure 7. Airflow distribution of eight-azimuth orientation at different layers of *H. rhamnoides* in spring (a), summer (b) and autumn (c).

4. Discussion

The downwind area of a single plant is a good place to study the airflow velocity distribution around the plant at different heights and different spacing behind the vegetation elements. It was beneficial to explore the effective protection length behind a plant and a sensible interval between plants to guide the selection of the density of sand-fixing vegetation. The plant porosity, height, number of rows (for a forest belt), arrangement, and spacing significantly influence the downwind airflow fields [4,12]. However, we were only interested in the airflow behind a single plant. With the space behind the plant increasing, the obstruction of the airflow gradually decreases, and airflow speed increases to a certain value similar to that in front of the plant. The effective protective length of the plant reaches a maximum downwind of vegetation (L_{max}), which is also the suitable interval for afforestation [30]. For plantation forests with a spacing between plants or rows of more than twice plant height, severe wind erosion occurs outside the maximum protective length, at the same time, roots and stems are seriously buried, resulting in increased mortality of plantations and reactivation of dunes. When the spacing of plants is too small, the cost of afforestation is too high, and community biodiversity is reduced [24]. It has been shown that airflow velocity is fully recovered 7 H downwind, and the downwind protective wake extends to approximately 7–10 H, as it does for a single plant in a wind tunnel experiment [5,6]. However, in this study, the maximum windproof length for a single plant was 1.0 H to 1.8 H due to the plant arrangement and spacing. *H. rhamnoides* had an average height of 1.0 m and the afforestation specification was 1. m \times 1.5 m in the study area. It can be seen that the afforestation specifications were matched with suitable intervals for afforestation in our study.

Airflow on each side of the plant showed a significant change in wind direction and velocity. Wind velocity in the frontal zone was 1.5 to 5.5 times that behind the plant, and about 1.0 to 1.2 times that to the side; there was a deflection from 0° to 90° from the side to the front (Figure 7). According to the airflow velocity simulation (Figure 6a), airflow generated creeping and skimming flow encountered obstacles, so it would form an elliptical speed-increasing zone between two plants or side and a cone-shaped wake zone behind plants. When spacing between two plants was smaller than the radius of two plant-side speed-increasing zones, a “corridor” airflow acceleration area was easily formed between plants and become a high-speed area of airflow movement. The smaller the difference in velocity for different orientations of plant, the smaller the difference in erosion around the plant, and the more balanced erosion morphology formed below the plant. In wind tunnel experiments, the sidewall effect on the airflow around the plant was so weak that it could be ignored [12]. However, the acceleration of plant-side airflow was the main driving force for micro landforms such as interplant erosion grooves and long-tail nebkhas behind the plant in the alpine desert [31]. Although it was difficult to generate erosion on the surface as sand-fixing plants grow year after year [24], *H. rhamnoides* experienced moderate erosion and accumulation as the wind direction changed seasonally, which promoted the formation of nebkhas due to the airflow field around shrubs.

The response of the plant community to aeolian activity was mainly reflected in the nebkha morphology of sand-fixing plants, the protection length behind the plants, the surface roughness, and the threshold wind velocity for sand movement [5,27]. The airflow behind the plants at different layers showed obvious differences in flow velocity and maximum protection length, while the range of low-value areas behind the plants increased as the plant height increased, and the decrease rate of the lowest velocity (R) in the lower layer was 25% to 90%. The airflow movement between adjacent plants was the result of the reduction in wind and weakening wind erosion by plants, as well as a mechanism to reveal the different azimuth of wind erosion intensity in communities. With equidistant rows and uniformly distributed plants on dunes, the direction of airflow movement between adjacent plants was different from that on a mobile dune. Clockwise deviation was the main direction in the upper layer, and was larger than that of the lower layer. A significant umbrella-shaped or dome-shaped sand pile was formed under *H. rhamnoides*, which caused the air-blocking effect in the low layer to be stronger than that in the upper layer. According to the magnitude of the deflection amplitude of the airflow

(Table 2), the areas to the side of the plant in the upper layer and behind the plant in the lower layer tend to have a larger direction change, and it was easy to generate circulation reflux and vortex.

The effectiveness of sand-fixing plant communities depends on the terrain, atmosphere, soil, and hydrology in which they are located. They also maintain their reproduction and succession by improving the habitat conditions of communities. In the sand-fixing community, plants reduce wind through the barrier effect and the swinging of branches and leaves. They encourage sand fixation and soil formation through their root system and rely on unique physiological functions to resist stresses such as drought, low temperature, wind, and storms, thereby improving the soil and microclimate and promoting natural vegetation restoration [32]. This positive feedback effect of ecological restoration is the fundamental aim of the desertification control project. *H. rhamnoides* has a higher porosity coefficient on the windward side and a lower flexibility of leaves, so that a significant acceleration of airflow was observed in the plant communities. However, the impact of vegetation on flow turbulence remains poorly understood, especially in field situations where the dynamic complexity of the flow structures cannot be controlled in the same way as in modeled or wind tunnel environments [6,33]. Live plants are far more complicated to control in terms of their appearance and behavior than artificial ones [18], and characterizing the flow around live plants that are porous, pliable, and of diverse geometry is significantly more complex [16].

In alpine deserts, wind-breaking and sand-fixing are the primary goals of desertification control, while soil improvement and natural vegetation restoration are the ultimate goals. The ecological restoration function of plants is based on the protection and soil improvement mechanisms of different plant species, and is the major aim of sand-fixing and other technologies of desertification control [34]. The windbreak and sand-fixing benefits of plant stands are based on the adaptability of plants. So, it is necessary to study the relationships between the wind-sand profile, the effective protection length, and the threshold wind velocity for sand movement and rate of sand transport based on plant growth and physiological characteristics. Because of changeable climatic conditions and limited field observations, long-term sequential monitoring of the wind and sand protection benefits of different species is needed. This can be used to more accurately assess ecological functions and optimize the sand-fixing performed by plant species in an alpine desert.

5. Conclusions

Sand-fixing plant areas reduce the wind speed increase below the canopy and increase the effective protective distance of plants, thereby strengthening the effect of airflow attenuation in the community and generating a low wind regime environment in order to reduce surface wind erosion in an alpine desert. The effective protection length of the sublayer of *H. rhamnoides* was 1.0 to 1.8 m under a density of 1.5 m square as the incoming wind speed was 8 m/s in an alpine desert. Wind velocity downwind of *H. rhamnoides* increased with increased height, while the airflow decreases rate (R) decreased in the sublayer and increased in the middle layer with increasing plant height. The airflow decreases rate (R) was negative in the upper layer as it decreased as plant height increased. Although different wind directions dominated in different seasons, it can be seen that the front and side of the plants were more affected by the wind direction, the same as the standard point; the side was slightly smooth, while the area behind was affected by multidirectional airflow, which had weak wind velocity and an unstable wind direction. The sand-fixing shrub *H. rhamnoides* showed a significant windproof function, especially when combined with previous studies in this area [25,26,29], and the 1.5 m square interval density of *H. rhamnoides* makes it suitable for alpine deserts.

Author Contributions: Conceptualization, L.T.; methodology, W.W.; software, W.W.; validation, D.Z. and L.T.; formal analysis, W.W.; data curation, W.W.; writing—original draft preparation, L.T.; writing—review and editing, L.T. and Y.Y.; visualization, D.Z.; supervision, D.Z.; project administration, L.T.; funding acquisition, L.T. and D.Z. All authors have read and agreed to the published version of the manuscript.

Funding: This research was funded by [Natural Science Foundation of China] grant number [41961017, 41661001], Qinghai Three Rivers Ecological Protection and Construction Phase II [2018-S-1], Science and Technology Project of Qinghai Province [2018-NK-A3] and Thousand High Innovative Talents Program of Qinghai Province [2016] .

Acknowledgments: Thanks for Mingyuan Zhang and Xin Zhou kindly help in field experiments.

Conflicts of Interest: The authors declare no conflict of interest.

References

- Dong, Z.B.; Fryrear, D.W.; Gao, S.Y. Modeling the roughness effect of blown-sand controlling standing vegetation in wind tunnel. *J. Desert Res.* **2000**, *20*, 260–263.
- Li, X.R.; Zhou, H.Y.; Wang, X.P.; Liu, L.C.; Zhang, J.G.; Chen, G.X.; Zhang, Z.S.; Liu, Y.B.; Tan, H.J.; Gao, Y.H. Ecological restoration and recovery in arid desert regions of China: A review for 60-year research progresses of Shapotou Desert Research and Experiment Station, Chinese Academy of Sciences. *J. Desert Res.* **2016**, *36*, 247–264.
- van de Ven, T.A.M.; Fryrear, D.W.; Spaan, W.P. Vegetation characteristics and soil loss by wind. *J. Soil Water Con.* **1989**, *44*, 347–349.
- Wolfe, S.A.; Nickling, W.G. The protective role of sparse vegetation in wind erosion. *Prog. Phys. Geogr.* **1993**, *17*, 50–68. [[CrossRef](#)]
- Leenders, J.K.; van Boxel, J.H.; Sterk, G. The effect of single vegetation elements on wind speed and sediment transport in the Sahelian zone of Burkina Faso. *Earth Surf. Process. Landf.* **2007**, *32*, 1454–1474. [[CrossRef](#)]
- Mayaud, J.R.; Wiggs, G.F.; Bailey, R.M. Characterizing turbulent wind flow around dryland vegetation. *Earth Surf. Process. Landf.* **2016**, *41*, 1421–1436. [[CrossRef](#)]
- Bagnold, R.A. *The Physics of Windblown Sand and Desert Dunes*; Methuen: London, UK, 1941; pp. 265–266.
- Leenders, J.K.; Sterk, G.; Van Boxel, J.H. Modelling wind-blown sediment transport around single vegetation elements. *Earth Surf. Process. Landf.* **2011**, *36*, 1218–1229. [[CrossRef](#)]
- Wu, X.X.; Zou, X.Y.; Zhou, N.; Zhang, C.L.; Shi, S. Deceleration efficiencies of shrub windbreaks in a wind tunnel. *Aeolian Res.* **2015**, *16*, 11–23. [[CrossRef](#)]
- Dong, Z.B.; Luo, W.Y.; Qian, G.Q.; Lu, P. Wind tunnel simulation of the three-dimensional airflow patterns around shrubs. *J. Geophys. Res. Earth Surf.* **2008**, *113*. [[CrossRef](#)]
- Okin, G.S. A new model of wind erosion in the presence of vegetation. *J. Geophys. Res. Earth Surf.* **2008**, *113*. [[CrossRef](#)]
- Cheng, H.; He, W.W.; Liu, C.C.; Zou, X.Y.; Kang, L.Q.; Chen, T.L.; Zhang, K.D. Transition model for airflow fields from single plants to multiple plants. *Agric. For. Meteorol.* **2019**, *266–267*, 29–42. [[CrossRef](#)]
- Wu, T.G.; Yu, M.K.; Wang, G.; Wang, Z.X.; Duan, X.; Dong, Y.; Cheng, X.R. Effects of stand structure on wind speed reduction in a *Metasequoia glyptostroboides* shelterbelt. *Agrofor. Syst.* **2013**, *87*, 251–257. [[CrossRef](#)]
- Li, X.R.; Zhang, Z.S.; Huang, L.; Wang, X.P. Review of the ecohydrological processes and feedback mechanisms controlling sand-binding vegetation systems in sandy desert regions of China. *Chin. Sci. Bull.* **2013**, *58*, 1483–1496. [[CrossRef](#)]
- Dong, Z.B.; Gao, S.Y.; Fryrear D., W. Drag coefficients, roughness length and zero-plane displacement height as disturbed by artificial standing vegetation. *J. Arid Environ.* **2001**, *49*, 485–505. [[CrossRef](#)]
- Mayaud, J.R.; Webb, N.P. Vegetation in drylands: Effects on wind flow and aeolian sediment transport. *Land* **2017**, *6*, 6. [[CrossRef](#)]
- Hesp, P.A. The formation of shadow dunes. *Sediment. Petrol.* **1981**, *51*, 101–112.
- Burri, K.; Gromke, C.B.; Lehning, M.; Graf, F. Aeolian sediment transport over vegetation canopies: A wind tunnel study with live plants. *Aeolian Res.* **2011**, *3*, 205–213. [[CrossRef](#)]
- Yang, H.; Lu, Q.; Wu, B.; Yang, H.; Zhang, J.; Lin, Y. Vegetation diversity and its application in sandy desert revegetation on Tibetan Plateau. *J. Arid Environ.* **2006**, *65*, 619–631. [[CrossRef](#)]
- Ni, J.R.; Li, Z.S.; Mendoza, C. Vertical profiles of aeolian sand mass flux. *Geomorphology* **2002**, *49*, 205–218. [[CrossRef](#)]

21. Liu, C.C.; Zheng, Z.Q.; Cheng, H.; Zou, X.Y. Airflow around single and multiple plants. *Agric. For. Meteorol.* **2018**, *252*, 27–38. [[CrossRef](#)]
22. Cheng, H.; Zhang, K.D.; Liu, C.C.; Zou, X.Y.; Kang, L.Q.; Chen, T.L.; He, W.W.; Fang, Y. Wind tunnel study of airflow recovery on the lee side of single plants. *Agric. For. Meteorol.* **2018**, *263*, 362–372. [[CrossRef](#)]
23. Wu, W.Y.; Zhang, D.S.; Tian, L.H.; Zhang, M.Y.; Zhou, X. Features of artificial plant communities from the east sand region of the Qinghai Lake over the last 10 years. *Acta Ecol. Sin.* **2019**, *39*, 2109–2121.
24. Wu, W.Y.; Zhang, D.S.; Tian, L.H.; Zhang, M.Y.; Zhou, X. Ecological responses of *Hippophae rhamnoides* to wind-sand hazard in alpine sand land. *Bul. Soil Water Con.* **2018**, *38*, 1–7.
25. Yu, Y.; Jia, Z.Q. Changes in soil organic carbon and nitrogen capacities of *Salix cheilophila* Schneid. along a revegetation chronosequence in semi-arid degraded sandy land of the Gonghe Basin, Tibetan Plateau. *Solid Earth* **2014**, *5*, 1045–1054. [[CrossRef](#)]
26. Wu, H.W.; Li, X.Y.; Jiang, Z.Y.; Chen, H.Y.; Zhang, C.C.; Xiao, X. Contrasting water use pattern of introduced and native plants in an alpine desert ecosystem, Northeast Qinghai-Tibet Plateau, China. *Sci. Total Environ.* **2016**, *542*, 182–191. [[CrossRef](#)]
27. Wu, W.Y.; Zhang, D.S.; Tian, L.H.; Zhang, M.Y.; Zhou, X. Morphologic features and forming causes of plant sandpiles in alpine sand land. *Arid Zone Res.* **2018**, *35*, 713–721.
28. Wang, H.J.; Tian, L.H.; Zhang, D.S.; Wu, W.Y.; Zhang, M.Y.; Zhang, H.W.; Wang, Q.Y.; Zhou, X. Characteristics of blown sand activities in sandy land on the eastern shore of the Qinghai Lake of China. *J. Desert Res.* **2020**, *40*, 49–56.
29. Wiggs, G.F.S.; Weaver, C.M. Turbulent flow structures and aeolian sediment transport over a barchan sand dune. *Geophys. Res. Lett.* **2012**, *39*, 1–7. [[CrossRef](#)]
30. Zhao, C.Y.; Yao, Z.Y.; Xue, X. Review on the research in influence of near surface sand flow on psammophilous and psammophilous vegetation. *J. Desert Res.* **2014**, *34*, 1307–1312.
31. Zuazo, V.H.D.; Pleguezuelo, C.R.R. Soil-erosion and runoff prevention by plant covers. *Agron. Sustain. Dev.* **2008**, *28*, 65–86. [[CrossRef](#)]
32. Zhao, Y.L.; Zhou, G.Y.; Chen, G.C. Sandy vegetation and its characteristics in east of Qinghai Lake area. *J. Desert Res.* **2007**, *27*, 820–825.
33. Clifford, N.J.; French, J.R. Monitoring and modelling turbulent flows: Historical and contemporary perspectives. In *Turbulence: Perspectives on Flow and Sediment Transport*; Clifford, N.J., French, J.R., Hardisty, J., Eds.; John Wiley & Sons: New York, NY, USA, 1993; pp. 1–34.
34. Onoda, Y.; Anten, N.P.R. Challenges to understand plant responses to wind. *Plant Signal. Behav.* **2011**, *6*, 1057–1059. [[CrossRef](#)]



© 2020 by the authors. Licensee MDPI, Basel, Switzerland. This article is an open access article distributed under the terms and conditions of the Creative Commons Attribution (CC BY) license (<http://creativecommons.org/licenses/by/4.0/>).